DALTON

Kinetics of oxidation of nitrogen(III) by an oxo-bridged dinuclear manganese(III,IV) complex in weakly acidic media

Shibnath Kundu, Anup Kumar Bhattacharya and Rupendranath Banerjee *

Department of Chemistry, Jadavpur University, Calcutta 700 032, India

The heterovalent oxo-bridged dinuclear manganese(III,IV) complex $[Mn_2O_2(phen)_4]^{3+}$ **1** aquates to $[Mn_2O_2(phen)_3(H_2O)_2]^{3+}$ **2** (phen = 1,10-phenanthroline) in phen–Hphen$^+$ buffer (pH 4–5). The equilibrium constant for the reaction was kinetically evaluated as $K_{1H} = 35 \pm 10$. Nitrite ion formed adducts **1N** and **2N** with **1** and **2** respectively. Their respective association constants, $K_{1N} = 14.1 \pm 2$ dm^3 mol^{-1} and $K_{2N} = 50 \pm 10$ dm^3 mol^{-1}, are small and indicate the outer-sphere nature of the adducts. Adduct **2N** is reduced *via* one-electron steps, ultimately to Mn^{II} with a rate constant $k_{2N} = (3.33 \pm 0.6) \times 10^{-2}$ s^{-1} at 30.0 °C and $I = 0.10$ mol dm^{-3} for the first step. No kinetic activity of **1N** was detectable under the experimental condition employed. Added Mn^{2+} has been found to scavenge phen from the reaction media and thus promotes the formation of **2N** and hence the reaction rate.

For the manganese aggregate in the oxygen-evolving complex (MnOEC) of photosystem II[1–7] the 16-line EPR spectrum and the short Mn–Mn distance of 2.70 Å are both consistent with minimally a dinuclear formulation with a $\{Mn_2O_2\}^{3+}$ core which is found, for example, in the complexes $[(phen)_2Mn^{III}O_2Mn^{IV}(phen)_2]^{3+}$ **1** (phen = 1,10-phenanthroline) and its analogue $[(bipy)_2Mn^{III}O_2Mn^{IV}(bipy)_2]^{3+}$ **1a** (bipy = 2,2′-bipyridyl).[2,8,9] Complexes **1** and **1a** are, therefore, considered as a paradigm of a preliminary or 'first generation' model[10] for MnOEC. Complexes with a $\{Mn_2O_2\}^{3+}$ core also form the basic units for Klein's tetrameric model[11–13] according to which MnOEC consists of a dimer of di-oxo-bridged dimers, a linked pair of $\{Mn_2O_2\}^{3+}$ cores. In between the dimer and tetramer models lies Hansson's trimer model,[14] which incorporates a mononuclear manganese(IV) species in electron-transfer equilibrium with a mixed-valence cluster. In this model too the mixed-valence cluster could be dinuclear like **1** and **1a**.

Apart from their significance as MnOEC models, the higher-valent dinuclear complexes of Mn are novel oxidants, useful for investigating the detailed kinetics and mechanism of electron-transfer reactions in higher-valent, multinuclear manganese systems. Investigations of this kind are rare[15,16] and we therefore report the kinetics of reaction of **1** with NO_2^- as a part of our continued interest in the kinetics of reactions of higher-valent metal complexes.[17,18]

Experimental

Materials

The complex $[(phen)_2Mn^{III}O_2Mn^{IV}(phen)_2][ClO_4]_3\cdot Me_2CO$ **1** was prepared according to the literature.[8] The crude dimer was dissolved in the minimum volume of acetone at room temperature (≈27 °C) and filtered. To the filtrate was added an equal volume of 0.01 mol dm^{-3} aqueous phenanthroline buffer (pH 4.5). The mixture was stored at < 5 °C for 48 h. Black crystals were deposited and washed with ice-cold acetone. They were stored over $CaCl_2$ in a vacuum desiccator at room temperature until constant weight. During this time the acetone of crystallisation is completely lost, as indicated by the disappearance of a prominant C–O stretching band at 1620 cm^{-1}. The kinetics was studied on the desiccated sample, which gave satisfactory elemental analyses and UV/VIS spectra in accord with the literature (literature values[8] of ε were corrected for the change in molecular weight due to loss of acetone during desiccation) {Found: C, 49.8; H, 2.7; Mn, 9.5; N, 9.7. Calc. for $C_{48}H_{32}Cl_3Mn_2N_8O_{14}$: C, 49.65; H, 2.8; Mn, 9.45; N, 9.65%}. Recrystallisation at 70 °C according to the literature method causes extensive decomposition and was, therefore, avoided.

Solutions of $NaNO_2$ (G.R., E. Merck), $NaNO_3$ (A.R., S.D.) and $Mn(NO_3)_2$ (G.R., E. Merck) were standardised as described earlier.[16,19] α-naphthylamine (G.R., Loba) (**CAUTION**: the amine should not contain β-naphthylamine, which is carcinogenic), sulfanilamide (G.R., Loba) and 1,10-phenanthroline (G.R., E. Merck) were used as provided. Reagent-grade chemicals, chromium(II)-scrubbed nitrogen gas and doubly distilled water were used. The disodium salt of 1,8-hydroxynaphthalene-3,6-disulfonic acid (chromotropic acid, A.R., BDH) was appropriately purified using activated charcoal and crystallisation from aqueous H_2SO_4.

Physical measurements and kinetics

The EPR spectra were recorded with a Varian EPR 4 X-band spectrometer having the following instrumental settings: field, 0.3 T; scan range, 0.8 T; gain, 6.3 × 10^3. The reaction kinetics was monitored *in situ* in thermostatted (30.0 °C) 1 cm quartz cells of a Shimadzu (UV-240) spectrophotometer. The ionic strength was generally maintained at 0.1 mol dm^{-3} ($NaNO_3$). 1,10-Phenanthroline has limited solubility at higher ionic strengths and at pH > 5; its solubility further decreases in perchlorate media where complex **1** also has poor solubility. Perchlorate media was therefore avoided. Solutions were weakly buffered with phen–Hphen$^+$ mixtures, the total 1,10-phenanthroline concentration, $c_{phen}(= [phen] + [Hphen^+])$, being in the range 0.004–0.010 mol dm^{-3}. Under the experimental conditions, the final manganese-containing species is mostly $[Mn(phen)]^{2+}$ (aq) and practically no free phen is released into the media. Hence even a weak buffering can control the pH change within ± 0.02 unit during the course of reactions.

Solution pH were measured with a model 335 pH meter (Systronics, India) using a calibrated electrode.[18] All kinetic experiments were made within the relatively narrow range pH 4–5 because of the solubility problems noted above. Again, in solutions with pH < 4 complex **1** undergoes complicated reactions, including oligomerisation, for which quantitative equilibrium data are not available. Hence it is difficult to interpret kinetic data at low pH. Pseudo-first-order conditions with the reductant in excess were maintained in all kinetic experiments. Complex concentration was generally 0.4 mmol dm^{-3}. Some solutions were rigorously deaerated with purified dinitrogen. Additional experiments were made in the presence of added $Mn(NO_3)_2$, at ionic strengths other than 0.10 mol dm^{-3} and complex concentrations other than 0.4 mmol dm^{-3}. Reactions were monitored mostly at 410 nm and occasionally at 525, 684 and 830 nm. No measurements were made at $\lambda < 410$ nm where NO_2^- absorbs strongly.

Stoichiometric measurements

The reaction stoichiometry was determined by spectrophotometric titration[16] of the oxidant complex **1** with $NaNO_2$. That in the presence of an excess of reductant was determined by measuring unreacted NO_2^- spectrophotometrically. The Griess–Ilsovey reaction was used as described earlier.[16]

The NO_3^- ion produced in the reaction of complex **1** with an excess of $NaNO_2$ was quantified spectrophotometrically by the chromotropic acid method,[20] the reactions between **1** and NO_2^- being carried out at pH 4.1–4.9 and $c_{phen} = 6 \times 10^{-3}$ mol dm^{-3}. The product solution was freed from Mn^{II} by eluting through a Dowex 50W X8 cation-exchange resin bed in the Na^+ form. Nitrite was removed by addition of a sulfite–urea solution.[20] The chromotropic acid reagent was then added followed by concentrated H_2SO_4. The yellow colour which developed due to NO_3^- did not interfere with NO_2^-. Its absorbance was measured at 410 nm to quantify NO_3^-; phen and bipy do not interfere with this method.

Results and Discussion

Stoichiometry and reaction products

Spectrophotometric titration (Fig. 1), measurements of unspent NO_2^- (Table 1) and the amount of NO_3^- produced (Table 2) all indicated a 2:3 stoichiometry with no loss of nitrogen from the reaction media. The overall reaction thus appears to be as in equation (1).

$$2[Mn^{III}O_2Mn^{IV}]^{3+} + 3NO_2^- + 2H^+ \longrightarrow 4Mn^{2+} + 3NO_3^- + H_2O \quad (1)$$

Solution equilibria

We have recently shown[16] that in aqueous acidic media $[Mn_2O_2(bipy)_4]^{3+}$ **1a** may undergo extensive acid-catalysed aquation, oxo-bridge protonation, dimer cleavage, disproportionation and core rearrangement. However, in the range pH 4.0–6.0 maintained with an excess of bipy–$Hbipy^+$ buffer only two manganese species co-exist as in equation (2). This is

$$[Mn_2O_2(bipy)_4]^{3+} + H^+ + 2H_2O \rightleftharpoons [Mn_2O_2(bipy)_3(H_2O)_2]^{3+} + Hbipy^+ \quad (2)$$

corroborated by the work of Manchanda *et al.*[21] The solution chemistry of **1** and **1a** is very similar and they exhibit almost identical spectral behaviour in solution.[8] It may be safely assumed for **1** that, under our experimental conditions of pH and c_{phen}, only equilibrium (3) is important.

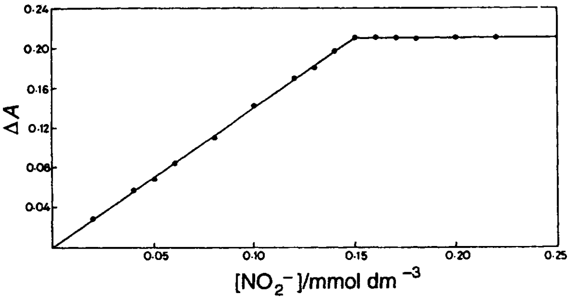

Fig. 1 Spectrophotometric titration of $[Mn_2O_2(phen)_4]^{3+}$ with NO_2^-: [complex] = 0.10 mmol dm^{-3}, $c_{phen} = 6.0 \times 10^{-3}$ mol dm^{-3}, $I = 0.10$ mol dm^{-3} ($NaNO_3$) and pH 4.5

$$[Mn_2O_2(phen)_4]^{3+} + H^+ + 2H_2O \overset{K_{1H}}{\rightleftharpoons} [Mn_2O_2(phen)_3(H_2O)_2]^{3+} + Hphen^+ \quad (3)$$

However, the spectral changes due to equilibrium (3) are small and spectrophotometric determination of K_{1H} is not possible. A similar situation was found[8,16] for equilibrium (2). Nevertheless, K_{1H} could be evaluated kinetically and the value is useful for mechanistic conclusions discussed later.

Kinetics

The reactions exhibit excellent first-order kinetics at least up to 90% completion at the monitoring wavelengths, *viz.* 410, 525, 684 and 830 nm. The first-order rate constants, k_0, under different conditions are collected in Tables 3 and 4.

Brewer *et al.*[9] have established an intervalence charge transfer as the origin of the absorption band of complex **1** in the near-infrared region. This band is a characteristic of all known Robin and Day class II[22] higher-valent dimanganese complexes containing a $\{Mn_2O_2\}^{3+}$ core. The corresponding isovalent $\{Mn^{III}O_2Mn^{III}\}$ dimer should, therefore, be optically transparent at 830 nm and this is actually seen for $[Mn_2O(O_2CMe)_2(bipy)_2(H_2O)_2]^{2+}$ and analogous Mn^{III}_2 complexes.[23] We have observed first-order kinetics at all λ and that the k_0 values measured at 830 nm are the same as those measured at lower wavelengths covering the ligand-to-metal charge-transfer (l.m.c.t.) regions and d–d bands, where both $\{Mn^{III}O_2Mn^{IV}\}$ and $\{Mn^{III}O_2Mn^{III}\}$ species absorb.

The observed exponential profile plus the invariance of k_0 with λ together with the absence of any absorbance drop immediately after mixing tell us simply that k_0 is determined by the first electron-transfer act, that subsequent steps are rapid and therefore kinetically silent. Typical six-line EPR spectra for Mn^{II} appear in the course of the reaction and indicate Mn^{II} as the final product.

Table 1 Stoichiometry* of reduction of $[(phen)_2Mn^{III}O_2Mn^{IV}(phen)_2]^{3+}$ by NO_2^-: estimation of unchanged $[NO_2^-]$

$[Mn^{III}Mn^{IV}]$/ mmol dm^{-3}	$[NO_2^-]$/ mmol dm^{-3}	pH	$\Delta[Mn^{III}Mn^{IV}]/\Delta[NO_2^-]$
0.20	0.80	4.9	0.69
0.50	2.00	4.2	0.64
0.50	2.00	4.95	0.66
0.50	1.50	4.90	0.68
0.60	2.50	4.70	0.71
0.80	2.00	4.90	0.70
			Average 0.68 ± 0.04

* Reactions were carried out at 30.0 °C in 6.0 mmol dm^{-3} phen–$Hphen^+$ buffer systems and at $I = 0.1$ mol dm^{-3} ($NaNO_3$). The media were deaerated by passage of purified dinitrogen.

Table 2 Stoichiometry* of reduction of $[(phen)_2Mn^{III}O_2Mn^{IV}(phen)_2]^{3+}$ by NO_2^-: estimation of NO_3^- produced

$[Mn^{III}Mn^{IV}]$/ mmol dm^{-3}	$[NO_2^-]$/ mmol dm^{-3}	pH	$\Delta[Mn^{III}Mn^{IV}]/\Delta[NO_3^-]$
0.1	0.40	4.1	0.67
0.2	0.60	4.4	0.69
0.4	2.00	4.6	0.65
0.5	1.50	4.6	0.64
0.6	2.00	4.8	0.67
0.7	2.50	4.9	0.69
			Average 0.66 ± 0.03

* Conditions similar to those in Table 1.

Table 3 Representative kinetic data[a] for reduction of $[Mn_2O_2(phen)_4]^{3+}$ with NO_2^-

pH	10^3c_{phen}/mol dm^{-3}	$10^3[NO_2^-]^b$/mol dm^{-3}	10^3k_0/s^{-1}
4.09	6.00	7.37	3.72 (3.69)
4.16		7.48	3.41 (3.36)
4.20		7.53	3.28 (3.21)
4.39		7.69	2.63 (2.56)
4.43		7.71	2.42 (2.43)
4.50		7.75	2.21 (2.23)
4.57		7.79	2.00 (2.05)
4.62		7.81	1.98 (1.93)
4.83		7.88	1.57 (1.52)
4.96		7.91	1.39 (1.33)
4.00	4.00	7.27	4.91 (4.87)
	6.00		3.88 (3.98)
	7.00		3.62 (3.64)
	8.00		3.33 (3.35)
	8.00^c		3.38
	8.00^d		3.36
	9.00		3.09 (3.12)
4.10	4.00	11.1	6.05 (6.15)
	5.00		5.45 (5.51)
	6.00		5.03 (4.98)
	7.00		4.53 (4.54)
	8.00		4.15 (4.17)
	9.00		3.76 (3.83)
4.35	4.00	5.74	2.79 (2.76)
	5.00		2.44 (2.38)
	6.00		2.11 (2.10)
	6.00^c		2.15
	7.00		1.96 (1.89)
	8.00		1.68 (1.69)
	8.00^c		1.65
	8.00^d		1.71
	9.00		1.62 (1.54)
	10.00		1.43 (1.41)
4.44	4.00	9.65	3.83 (3.84)
	5.00		3.21 (3.30)
	6.00		2.89 (2.90)
	7.00		2.56 (2.59)
	8.00		2.38 (2.33)
	8.00^c		2.38
	9.00		2.12 (2.12)
	10.00		2.03 (1.95)
4.50	4.00	14.5	4.91 (4.92)
	5.00		4.25 (4.24)
	6.00		3.79 (3.72)
	6.00^c		3.76
	7.00		3.30 (3.32)
	8.00		2.98 (2.99)
	8.00^d		2.95
	9.00		2.69 (2.72)
	10.00		2.49 (2.51)
	4.00	7.75	3.06 (2.99)
	5.00		2.56 (2.56)
	6.00		2.32 (2.23)
	7.00		2.01 (1.98)
	8.00		1.78 (1.78)
	8.00^d		1.77
	8.00^c		1.83
	8.00^e		1.75
	9.00		1.57 (1.63)
	4.00	19.4	6.04 (6.04)
	5.00		5.37 (5.23)
	6.00		4.50 (4.60)
	7.00		4.17 (4.11)
	8.00		3.70 (3.71)
	8.00^e		3.67
	8.00^f		3.73
	9.00		3.34 (3.38)
4.98	4.00	4.95	1.19 (1.21)
	5.00		0.93 (1.00)
	6.00		0.88 (0.86)
	7.00		0.73 (0.75)
	8.00		0.61 (0.66)
	8.00^d		0.68
	8.00^f		0.63
	9.00		0.60 (0.62)
	10.00		0.54 (0.55)
4.50	5.00	19.4	5.27 (5.23)
		14.5	4.28 (4.23)
		9.69	3.11 (3.08)
		7.75	2.58 (2.56)
		5.82	2.06 (1.99)
	6.00	19.4	4.57 (4.60)
		19.4^d	4.59
		14.5	3.75 (3.72)
		9.69	2.78 (2.70)
		7.75	2.20 (2.23)
		5.82	1.75 (1.75)
	7.00	19.4	4.12 (4.11)
		19.4^e	4.15
		19.4^f	4.09
		14.5	3.33 (3.31)
		9.69	2.41 (2.40)
		7.75	1.99 (1.98)
		5.82	1.55 (1.54)
	8.00	19.4	3.68 (3.71)
		14.5^g	2.96
		9.69	2.20 (2.16)
		7.75	1.82 (1.78)
		5.82	1.42 (1.38)
	9.00	19.4	3.41 (3.39)
		14.5	2.73 (2.72)
		9.69	1.97 (1.96)
		7.75	1.59 (1.62)
		5.82	1.27 (1.25)

[a] Average of at least three experiments; standard deviation 2–5%. Reactions were carried out at 30.0 °C, [complex] = 0.4 mmol dm^{-3} and I = 0.10 mol dm^{-3} ($NaNO_3$) unless stated otherwise. Parenthetical values were calculated using equation (9). [b] $[NO_2^-]$ was calculated using $K_a = 10^{-3}$ mol dm^{-3} for HNO_2. [c] Reaction mixture purged with purified dinitrogen. [d] Measurements at 830 nm. [e] Measurements at 684 nm. [f] Measurements at 525 nm. All measurements except those marked with *d–f* were at 410 nm. [g] [complex] varied in the range 0.2–0.5 mmol dm^{-3}; k_0 varied within 2–5%.

Table 4 Effect of $[Mn^{2+}]$ and ionic strength, I, on k_0*

pH	I/mol dm^{-3}	$[NO_2^-]$/mmol dm^{-3}	$[Mn^{2+}]$/mmol dm^{-3}	10^3k_0/s^{-1}
4.45	0.50	7.73	0.00	0.99
	0.30			1.38
	0.20			1.61
	0.10			2.44
4.30	0.10	9.54	1.00	7.68
			0.50	5.05
			0.05	3.50

* [complex] = 0.4 mmol dm^{-3}, c_{phen} = 0.006 mol dm^{-3}, 30.0 °C; $[NO_2^-]$ was calculated from the pK_a value of HNO_2 ($K_a = 10^{-3}$ mol dm^{-3}) and the analytical concentration of $NaNO_2$.

Variation of k_0. Rate constant k_0 increases with increasing $[NO_2^-]$ but tends to saturate at higher $[NO_2^-]$ (Fig. 2). Plots of $1/k_0$ *vs.* $1/[NO_2^-]$ are excellent straight lines (r > 0.98) with finite intercepts (see Fig. 3). The rate constant also increases with $[H^+]$ and k_0 *vs.* $[H^+]$ plots are excellent straight lines with finite intercepts (Fig. 4); it also increases with increasing $[Mn^{2+}]$ but decreases with increasing ionic strength and c_{phen}; plots of $1/k_0$ *vs.* c_{phen} are excellent straight lines with finite intercepts. It does not change with a change in [complex] or when the reaction media are purged with purified dinitrogen.

Mechanism. The nature of the dependence of k_0 on c_{phen} indicates a pre-equilibrium step involving phen as a product.

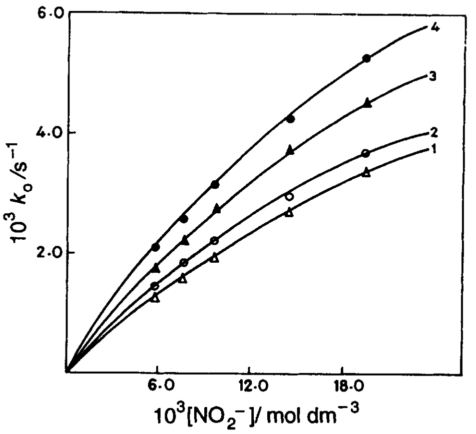

Fig. 2 Variation of k_0 with $[NO_2^-]$ at 30.0 °C: [complex] = 0.4 mmol dm^{-3}, I = 0.1 mol dm^{-3}, pH 4.5; c_{phen}/mmol dm^{-3} 9.0 (1), 8.0 (2), 6.0 (3) and 5.0 (4)

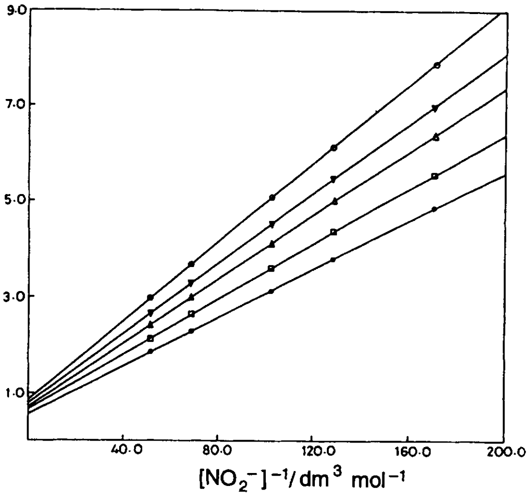

Fig. 3 Double reciprocal plots of $(k_0)^{-1}$ *vs.* $[NO_2^-]^{-1}$ at 30.0 °C: [complex] = 0.4 mmol dm^{-3}, pH 4.5, I = 0.10 mol dm^{-3}. c_{phen} = 5 × 10^{-3} (●), 6 × 10^{-3} (□), 7 × 10^{-3} (△), 8 × 10^{-3} (▽) and 9 × 10^{-3} mol dm^{-3} (○)

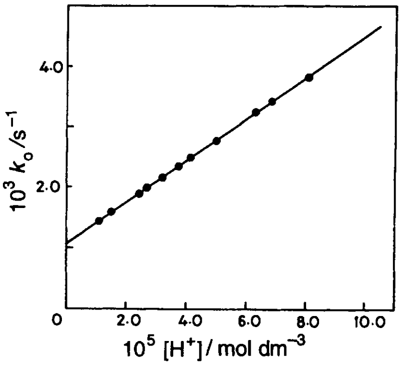

Fig. 4 Dependence of k_0 on [H$^+$] at 30.0 °C: [complex] = 0.4 mmol dm^{-3}, c_{phen} = 6.0 × 10^{-3} mmol dm^{-3}, $[NO_2^-]$ = 8.0 × 10^{-3} mol dm^{-3}, I = 0.10 mol dm^{-3}

The linearity of $1/k_0$ *vs.* $1/[NO_2^-]$ plots indicates formation of adduct(s) between NO_2^- and complex **1** or some of its derivatives. The acid dependence reveals that there is a derivative of **1** which is kinetically more active and which is formed from **1** in a proton-assisted pre-equilibrium step.

Nitrous acid generally reduces a substrate at a slower rate than NO_2^- and no evidence is available for kinetic superiority of HNO_2 over NO_2^- in weakly acidic media. Under our experimental conditions $[HNO_2] \ll [NO_2^-]$ (pK_a for HNO_2 is 3.0) and one can safely assume that $[HNO_2]$ is kinetically insignificant for the present study. On the basis of the above observations, Scheme 1 seems plausible.

$$\underset{\mathbf{1}}{[Mn_2O_2(phen)_4]^{3+}} + H^+ + 2H_2O \overset{K_{1H}}{\rightleftharpoons} \underset{\mathbf{2}}{[Mn_2O_2(phen)_3(H_2O)_2]^{3+}} + Hphen^+ \quad (3)$$

$$\mathbf{1} + NO_2^- \overset{K_{1N}}{\rightleftharpoons} \underset{\mathbf{1N}}{\{[Mn_2O_2(phen)_4]^{3+}{\cdot}NO_2^-\}} \quad (4)$$

$$\mathbf{2} + NO_2^- \overset{K_{2N}}{\rightleftharpoons} \underset{\mathbf{2N}}{\{[Mn_2O_2(phen)_3(H_2O)_2]^{3+}{\cdot}NO_2^-\}} \quad (5)$$

$$\mathbf{1N} \xrightarrow{k_{1N}} \text{products, ultimately Mn}^{II} \quad (6)$$

$$\mathbf{2N} \xrightarrow{k_{2N}} \text{products, ultimately Mn}^{II} \quad (7)$$

Scheme 1

Data analyses. Scheme 1 leads to equation (8) as the

$$k_0 = \frac{k_{1N}K_{1N}[NO_2^-]c_{phen} + k_{2N}K_{2N}K_{1H}[NO_2^-](K_a + [H^+])}{c_{phen} + K_{1H}(K_a + [H^+])(1 + K_{2N}[NO_2^-]) + K_{1N}c_{phen}[NO_2^-]} \quad (8)$$

expression for k_0. It was linearised[24] and solved for k_{1N}, k_{2N}, K_{1N}, K_{2N} and K_{1H} using the Lotus 123 spread sheet for simultaneous equations.[24] We used the known value of K_a, the acid dissociation constant (1.12 × 10^{-5} dm^3 mol^{-1}, I = 0.10 mol dm^{-3}, KNO_3)[25] for Hphen$^+$. The value thus found for k_{1N} is not statistically different from zero. Other kinetic parameters are K_{1N} = 14 ± 2 dm^{-3} mol^{-1}, K_{2N} = 50 ± 10 dm^3 mol^{-1}, K_{1H} = 35 ± 10 and k_{2N} = (3.33 ± 0.6) × 10^{-2} s^{-1}. Since $k_{1N} \approx 0$, equation (8) transforms to (9). Plots of $1/k_0$ *vs.* c_{phen}

$$1/k_0 = \frac{c_{phen}(1 + K_{1N}[NO_2^-])}{k_{2N}K_{2N}K_{1H}(K_a + [H^+])[NO_2^-]} + \frac{1 + K_{2N}[NO_2^-]}{k_{2N}K_{2N}[NO_2^-]} \quad (9)$$

(see Fig. 5) give m_1 as the slope [equation (10)]. The left-hand side of equation (10), when plotted as a function of $1/[NO_2^-]$

$$m_1 = \frac{1 + K_{1N}[NO_2^-]}{k_{2N}K_{2N}K_{1H}(K_a + [H^+])[NO_2^-]}$$

$$m_1(K_a + [H^+]) = \frac{1}{k_{2N}K_{2N}K_{1H}[NO_2^-]} + \frac{K_{1N}}{k_{2N}K_{2N}K_{1H}} \quad (10)$$

(see Fig. 6), produces $(k_{2N}K_{2N}K_{1H})^{-1}$ as the slope and K_{1N} as intercept/slope. The intercept of $1/k_0$ *vs.* c_{phen} is given by equation (11). A plot of I_1 *vs.* $1/[NO_2^-]$ (Fig. 7) produced k_{2N}

$$I_1 = \frac{1 + K_{2N}[NO_2^-]}{k_{2N}K_{2N}[NO_2^-]} = \frac{1}{k_{2N}K_{2N}[NO_2^-]} + \frac{1}{k_{2N}} \quad (11)$$

from intercept and K_{2N} from the intercept/slope. These values were used to extract K_{1H} from the value of $(k_{2N}K_{2N}K_{1H})^{-1}$, *i.e.* the slope of the plot of $m_1(K_a + [H^+])$ *vs.* $1/[NO_2^-]$.

Such graphically evaluated kinetic parameters agree closely with those obtained by the Lotus 123 spread sheet and they reproduce k_0 within 2–5%.

Nature of the adducts 1N and 2N. Association constants for some adducts[26–29] in aqueous media are collected in Table 5. It appears that K_{1N} and K_{2N} lie within the range for outer-sphere association constants of several +3/1 − type adducts. The values are much smaller than those for inner-sphere adducts

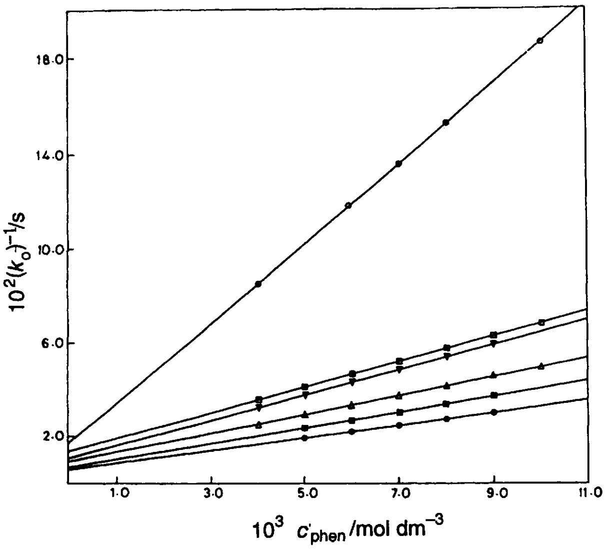

Fig. 5 Variation of k_0 with c_{phen} at different constant pH and $[NO_2^-]$: [complex] = 0.4 mmol dm^{-3}, I = 0.10 mol dm^{-3}, 30.0 °C. (●) pH 4.5, $[NO_2^-]$ = 19.4 × 10^{-3} mol dm^{-3}; (■) pH 4.5, $[NO_2^-]$ = 14.5 × 10^{-3} mol dm^{-3}; (△) pH 4.44, $[NO_2^-]$ = 9.65 × 10^{-3} mol dm^{-3}; (▽) pH 4.5, $[NO_2^-]$ = 7.75 × 10^{-3} mol dm^{-3}; (□) pH 4.35, $[NO_2^-]$ = 5.74 × 10^{-3} mol dm^{-3}; (○) pH 4.98, $[NO_2^-]$ = 4.95 × 10^{-3} mol dm^{-3}

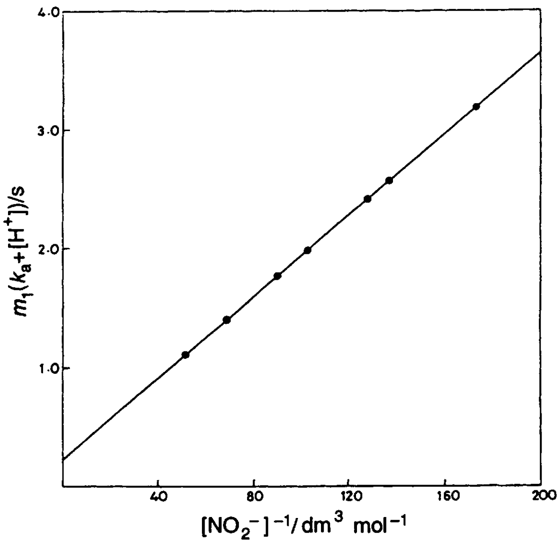

Fig. 6 Graphical evaluation of kinetic parameters at 30.0 °C: [complex] = 0.4 mmol dm^{-3}, I = 0.10 mol dm^{-3}

(10–12) formed by complexes reasonably comparable to $[Mn_2O_2(phen)_3(H_2O)_2]^{3+}$. The values for K_{1N} and K_{2N}, therefore, indicate the outer-sphere nature of **1N** and **2N**. Outer-sphere association constants may appreciably increase if there is a chance for hydrogen bonding between the interacting particles; entry 9 in Table 5 is a case in point. Hydrogen-bonding involving the co-ordinated water molecules is possible in **2N** but not in **1N**, and may explain why K_{2N} is larger than K_{1N}.

Kinetic superiority of adduct 2N over 1N. The results demonstrate an overwhelming kinetic dominance of the aquated species **2** over the parent complex **1**. We found a similar situation[16] in redox reactions of $[Mn_2O_2(bipy)_4]^{3+}$ with NO_2^-. Kinetic dominance of the aquated species over the parent complex is also well known in the redox reactions of mononuclear complexes of higher-valent manganese. This may be exemplified by $[Mn(H_2O)_2(acac)_2]^+$ (Hacac = acetylacetone), which completely swamps the kinetic activity of $[Mn(acac)_3]$ with its own while reacting with S^{IV},[18] glyoxalate,[30] oxalate[31] and $H_2PO_2^-$.[32] The crystal structure of **1** shows that the dinuclear complex belongs to the Robin and Day class II,[22] with deeply trapped valence. It is not surprising that **1** maintains the gross trends of reactivity observed for reasonably comparable mononuclear systems.

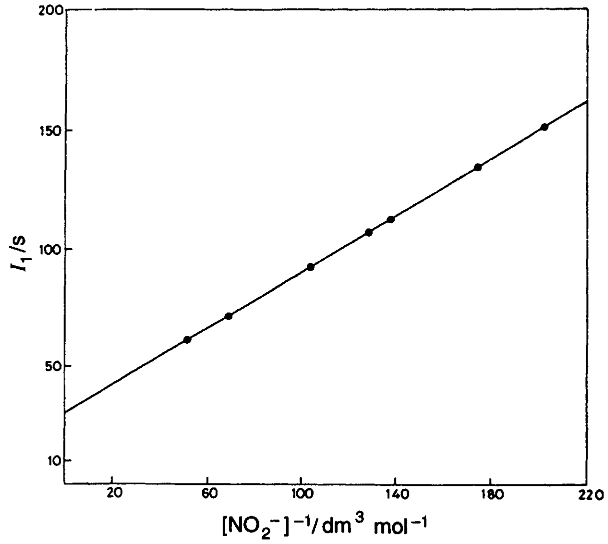

Fig. 7 Evaluation of K_{2N} and k_{2N} at 30.0 °C: [complex] = 0.4 mmol dm^{-3}, I = 0.10 mol dm^{-3}

Table 5 Association constants for some adducts[a]

No.[b]	Ion pair	Association constant/ dm^3 mol^{-1}	Ref.
1	$[Co(NH_3)_6]^{3+}$, Cl^-	74	26
2	$[Co(NH_3)_6]^{3+}$, Br^-	46	26
3	$[Co(NH_3)_6]^{3+}$, I^-	17	26
4	$[Co(NH_3)_6]^{3+}$, N_3^-	20	26
5	$[Co(en)_3]^{3+}$, N_3^-	11	26
6	$[Cr(H_2O)_6]^{3+}$, Cl^-	13	27
7	$[Mn_2O_2(phen)_4]^{3+}$, NO_2^-	14 (K_{1N})	This work
8	$[Mn_2O_2(phen)_3(H_2O)_2]^{3+}$, NO_2^-	50 (K_{2N})	This work
9	$[Mn_2O_2(bipy)_4]^{3+}$, $Hasc^-$	140	15
10	$[Mn(bipy)_2]^{3+}$ (aq), N_3^-	≈10^4[c]	28
11	$[Mn(acac)_2(H_2O)_2]^+$, $acac^-$	7.2 × 10^3	29
12	$[Mn_2O_2(phen)_2(H_2O)_2]^{3+}$, phen	3.6 × 10^3[d]	This work

en = Ethane-1,2-diamine, $Hasc^-$ = ascorbate. [a] I = 0 for entries 1–6; 0.1 mol dm^{-3} for 7–9 and 12; 1.0 mol dm^{-3} for 10; 0.2 mol dm^{-3} for 11; 25.0 °C for 1–6 and 9–11; 30.0 °C for 7, 8 and 12. [b] Cases 1–6 and 9 are known examples of outer-sphere adducts, 10–12 are inner-sphere complexes. [c] Calculated using data in ref. 28 and pK_a value of HN_3. [d] K_a/K_{1H}, where K_a is the acid-dissociation constant for $Hphen^+$.

One- vs. two-electron transfer. Equation (7) in Scheme 1 definitely represents a multistep process in which only the first act of electron transfer controls the measured k_0. All steps within (7) are likely to be one-electron changes, and all manganese species except Mn^{II} are considered to be dinuclear in line with (*a*) the work of Gould and co-workers,[15] (*b*) the proposed mechanism for the formation of $[Mn^{IV}_2(gluc)_4O_2(OH)_2]^{6-}$ (gluc = gluconate ion) from $[Mn^{II}_2(gluc)_4(H_2O)_2]^{4-}$ and O_2,[33] (*c*) the known stepwise one-electron reduction of $\{Mn_2O_2\}^{3+}$ cores at electrodes,[34,35] and (*d*) the well known tendency of manganese to form bis(μ-oxo) complexes. One interesting example of the propensity of manganese to form and retain the $\{Mn_2O_2\}^{n+}$ core is the isolation[9] of a complex with a *cis*-co-ordinated [14]aneN$_4$ ligand, which would normally co-ordinate in a planar *trans* geometry.[35–37] The marked stability of the $\{Mn_2O_2\}^{3+}$ dimer

Table 6 An approximate Marcus correlation for oxidation by dinuclear manganese(III, IV) complexes

Reductant	$k_{12}{}^a$/dm^3 mol^{-1} s^{-1}	k_{22}/dm^3 mol^{-1} s^{-1}	E_f(NHE)/V	$\log k_{12} - 0.5 \log k_{22}$	Ref.
$S_2O_3{}^{2-}$	24.5 (phen)	2.3×10^5 [43]	1.30[43]	−1.29	42
	17.2 (bipy)			−1.44	42
Hydroquinone	1.6×10^2 (bipy)	7×10^5 [44]	1.08[45]	−0.718	15
$NO_2{}^-$	34.9 (bipy)	0.30[43]	0.87[46]	1.80	16
	58.8 (phen)			2.29	This work
$HSO_3{}^-$	2.0×10^2 (bipy)	4.0[47]	0.72[47]	2.0	15
Ascorbate	1.2×10^5 (bipy)	3.5×10^5 [48]	0.71[48]	2.31	15

[a] k_{12} of refs. 15, 16 and 42 are $K_{2N}k_{2N}K_{1H}$ of this work.

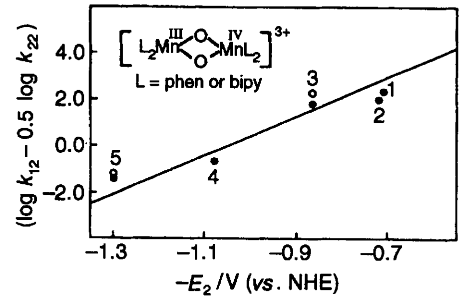

Fig. 8 An approximate Marcus cross-relation for (○) $[Mn_2O_2(phen)_4]^{3+}$ and (●) $[Mn_2O_2(bipy)_4]^{3+}$. Reductants: 1, $Hasc^-$; 2, $HSO_3{}^-$; 3, $NO_2{}^-$; 4, hydroquinone; 5, $S_2O_3{}^{2-}$

may be related to the presence of strong $Mn(d_\pi) \longleftarrow O^{2-}(p_\pi)$ mixing in the $\{Mn_2O_2\}^{n+}$.[38]

The dominance of one- over two-electron transfers, *e.g.* $Mn^{III}Mn^{IV} \longrightarrow Mn^{III}Mn^{II}$, is likely because the latter can occur only with a large activation barrier due to significant structural reorganisation, which $NO_2{}^-$ must undergo for concomitant formation of $NO_2{}^+$. Such a barrier would discourage a two-electron step.[39] It may be mentioned here that the different S-states (S_0–S_4) in Kok's model[40] for the MnOEC of photosystem II also involve one-electron changes.

A sequence of possible one-electron steps within equation (7), is (7a). This is preferred over (7b) for reasons discussed earlier.[16] The one-electron steps in equation (7a) should produce NO_2 as the immediate oxidation product which rapidly disproportionates to $NO_2{}^-$ and $NO_3{}^-$ ($k = 1.0 \times 10^8$ dm^3 mol^{-1} s^{-1} in water),[41] and NO_2 is neither a final product escaping as gas nor does it survive long enough for consumption by higher-valent manganese species.

$$Mn^{III}Mn^{IV} \longrightarrow Mn^{III}Mn^{III} \longrightarrow Mn^{III}Mn^{II} \longrightarrow 2Mn^{II} \qquad (7a)$$

$$Mn^{III}Mn^{IV} \longrightarrow Mn^{II}Mn^{IV} \longrightarrow \textit{etc.} \qquad (7b)$$

An approximate Marcus relation. If $f_{12} \approx 1$ then the Marcus cross-relation may be written as $\log k_{12} = 0.5 \log k_{11} + 0.5 (\log k_{22} + \log K_{12} + \log W_{12})$ or $(\log k_{12} - 0.5 \log k_{22}) = 0.5 (\log k_{11} + \log W_{12}) + (\Delta E/2 \times 0.059)$ where the terms have there usual significances and $\Delta E = E_1 - E_2$. The reduction potentials, E_1, are nearly the same for $[Mn_2O_2(phen)_4]^{3+}$ (0.30 V) and $[Mn_2O_2(bipy)_4]^{3+}$ (0.29 V *vs.* saturated calomel electrode, SCE). It is expected that the corresponding reduction potentials of the two aqua-complexes are also very similar. Assuming further that $\log k_{11}$ is similar for the two oxidants and $\log W_{12}$ remains fairly constant for the series of reactions, one expects a linear relation between $\log k_{12}$ and E_2, the formal reduction potentials for different reductants (see Table 6). Fig. 8 demonstrates such a relation using the data in Table 6. The straight line has been drawn with the theoretical slope 8.47 expected for an outer-sphere, one-electron-transfer reaction.

Effect of added Mn^{2+} ion. Added Mn^{2+} scavenges phen to form $[Mn(phen)]^{2+}$ (aq) in the experimental pH range. This thus indirectly drags the equilibrium (3) farther to the right and produces more of the kinetically active compound **2N**. This increases k_0 (Table 4). Such scavenging of phen by Mn^{2+} is also helpful in maintaining the pH of the reacting medium fairly fixed. A similar situation was observed[16] with **1a**.

Conclusion

An excess of phen–$Hphen^+$ buffer stabilises the complex $[Mn_2O_2(phen)_4]^{3+}$ **1** in aqueous solution. However, in such media, $NO_2{}^-$ reduces the diaqua derivative of **1** in an outer-sphere one-electron pathway. All subsequent redox steps are rapid and probably involve one-electron changes within the $\{Mn_2O_2\}^{n+}$ core. This behaviour is comparable to one-electron changes proposed in Kok's model. The diaqua derivative of **1** is kinetically much more active than its parent, a situation common to mononuclear manganese complexes, but previously unnoticed.

Acknowledgements

We gratefully acknowledge financial assistance from Department of Science and Technology (New Delhi) and University Grants Commision, and the award of a project assistantship to A. K. B. by U.G.C. We thank Mr. S. Mukherjee and Mr. T. Dutta of Bose Institute, Calcutta, for their assistance in EPR measurements.

References

1 M. W. Wemple, D. M. Adam, K. Fotting, D. W. Hendrickson and G. Christou, *J. Am. Chem. Soc.*, 1995, **117**, 7275 and refs. therein.
2 J. A. Kirby, A. S. Robertson, J. P. Smith, A. C. Thompson, S. R. Cooper and M. P. Klein, *J. Am. Chem. Soc.*, 1981, **103**, 5529.
3 R. J. Debus, *Biochim. Biophys. Acta*, 1992, **1102**, 269.
4 W. H. Armstrong, in *Manganese Redox Enzymes*, ed. V. L. Pecoraro, VCH, New York, 1992.
5 P. Joliot, G. Barbieri and R. Chabaud, *Photochem. Photobiol.*, 1969, **10**, 302.
6 G. W. Brudvig and R. H. Crabtree, *Proc. Natl. Acad. Sci. USA*, 1986, **83**, 4586.
7 K. Wieghardt, *Angew. Chem., Int. Ed. Engl.*, 1989, **28**, 1153.
8 S. R. Cooper and M. Calvin, *J. Am. Chem. Soc.*, 1977, **99**, 6623.
9 K. J. Brewer, M. Calvin, R. S. Lumpkin, J. W. Otvos and L. O. Spreer, *Inorg. Chem.*, 1989, **28**, 4446.
10 K. S. Hagen, W. H. Armstrong and H. Hope, *Inorg., Chem.*, 1988, **27**, 967.
11 V. K. Yachndra, V. J. DeRose, M. J. Latimer, I. Mukherji, K. Sauer and M. P. Klein, *Science*, 1993, **260**, 675.
12 P. Philouze, G. Blondin, J. J. Girerd, J. Guilhem, C. Pascard and D. Lexa, *J. Am. Chem. Soc.*, 1994, **116**, 8557.
13 K. Wieghardt, *Angew. Chem., Int. Ed. Engl.*, 1994, **33**, 725.
14 O. Hansson, R. Aasa and T. Vanngard, *J. Biophys.*, 1987, **51**, 825.
15 M. C. Ghosh, J. W. Reed, R. N. Bose and E. S. Gould, *Inorg. Chem.*, 1994, **33**, 73.
16 S. Chowdhuri, S. Mukhopadhyay and R. Banerjee, *J. Chem. Soc., Dalton Trans.*, 1995, 621.
17 R. Banerjee, *Proc. Indian Acad. Sci. (Chem. Sci.)*, 1994, **106**, 655 and refs. therein.

18 S. Mukhopadhyay and R. Banerjee, *J. Chem. Soc., Dalton Trans.*, 1993, 933 and refs. therein.
19 S. Mukhopadhyay and R. Banerjee, *J. Chem. Soc., Dalton Trans.*, 1994, 1349.
20 P. W. West and T. P. Ramachandran, *Anal. Chim. Acta*, 1966, **35**, 317.
21 R. Manchanda, G. W. Brudvig and R. H. Crabtree, *New J. Chem.*, 1994, **18**, 561.
22 M. B. Robin and P. Day, *Adv. Inorg. Chem. Rediochem.*, 1967, **10**, 247.
23 S. Menage, J. J. Girerd and A. Gleizes, *J. Chem. Soc., Chem. Commun.*, 1988, 431.
24 R. Banerjee, R. Das and A. K. Chakraburtty, *J. Chem. Soc., Dalton Trans.*, 1991, 987.
25 R. L. Gustafson and A. E. Martell, *J. Am. Chem. Soc.*, 1959, **81**, 525.
26 M. G. Evans and G.-H. Naucollas, *Trans. Faraday Soc.*, 1953, **49**, 363.
27 C. Postmus and E. L. King, *J. Phys. Chem.*, 1955, **59**, 1208.
28 M. P. Heyward and C. F. Wells, *J. Chem. Soc., Dalton Trans.*, 1988, 1331.
29 G. H. Cartledge, *J. Am. Chem. Soc.*, 1951, **73**, 4416.
30 R. Banerjee, R. Das and A. K. Chakraburtty, *J. Chem. Soc., Dalton Trans.*, 1990, 3277.
31 S. Mukhopadhyay, S. Kundu and R. Banerjee, *Proc. Indian Acad. Sci. (Chem. Sci.)*, 1995, **107**, 403.
32 R. Banerjee, R. Das and A. K. Chakraburtty, *Transition Met. Chem.*, 1992, **17**, 227.
33 M. E. Bodini and D. T. Sawyer, *J. Am. Chem. Soc.*, 1976, **98**, 8366.
34 L. Y. Martin, C. R. Sperati and D. H. Busch, *J. Am. Chem. Soc.*, 1977, **99**, 2968.
35 V. J. Thom, M. S. Shaikjee and R. D. Hancock, *Inorg. Chem.*, 1986, **25**, 2992.
36 C.-M. Che, W.-K. Cheng, T.-F. Lai, C.-K. Poon and T. C. W. Mak, *Inorg. Chem.*, 1987, **26**, 1678.
37 L. Fabbrizzi, *Comments Inorg. Chem.*, 1985, **4**, 33.
38 L. J. Boucher and C. G. Coe, *Inorg. Chem.*, 1975, **14**, 1289.
39 W. K. Wilmarth, D. M. Stanbury, J. E. Byrd, N. H. Po and C. Chua, *Coord. Chem. Rev.*, 1983, **51**, 155.
40 B. Kok, B. Forbush and M. McGloin, *Photochem. Photobiol.*, 1970, **11**, 457.
41 Y. N. Lee and S. E. Schwartz, *J. Phys. Chem.*, 1981, **85**, 840.
42 S. Kundu, B. Mondal and R. Banerjee, unpublished work.
43 R. Sarala and D. M. Stanbury, *Inorg. Chem.*, 1992, **31**, 2771.
44 E. Pelizzetti, E. Mentasti and E. Pramauro, *Inorg. Chem.*, 1978, **17**, 1181.
45 E. Pelizzetti and E. Mentasti, *J. Chem. Soc., Dalton Trans.*, 1976, 2222.
46 V. M. Berdnikov and N. M. Bazhin, *Russ. J. Phys. Chem.*, 1970, **44**, 395.
47 R. Sarala, M. A. Islam, S. B. Rabin and D. M. Stanbury, *Inorg. Chem.*, 1990, **29**, 1133.
48 M. J. Akhtar and A. Haim, *Inorg. Chem.*, 1988, **27**, 1608.

Received 2nd April 1996; *Paper* 6/02317G